The simulated seasonal variability of the Ku-band radar altimeter effective scattering surface depth in sea ice

R. T. Tonboe, S. Andersen, R. S. Gill
Danish Meteorological Institute, Lyngbyvej 100, DK-2100 Copenhagen Ø, Denmark
Tel.:+45 39 15 73 49, e-mail: rtt@dmi.dk

L. Toudal Pedersen
Ørsted, bld. 348, Technical University of Denmark, DK-2800 Kgs. Lyngby, Denmark

Keywords: Radar altimetry, sea ice, seasonal variation, radiative transfer modelling, effective scattering surface, radar penetration.

ABSTRACT: Radiative transfer simulations show that the Ku-band radar altimeter sea ice effective scattering surface depth is sensitive to snow density, thickness and the snow and ice surface roughness. In order to reduce the errors in sea ice freeboard estimation and the derived ice thickness to acceptable levels it will be necessary to have access to these snow and ice parameters. Here a thermodynamic and mass model is used to simulate the seasonal snow cover at 82.5ºN, 0.0ºE in the Arctic Ocean using the European Centre for Medium-range Weather Forecast (ECMWF) re-analysis meteorological data as input. The simulated seasonal snow profiles are used as input to a backscatter model. The seasonal variability of the effective scattering surface depth is discussed in terms of the simulated snow cover properties.

1 INTRODUCTION

Submarine sonar is widely used to measure sea ice thickness in the Arctic Ocean (Wadhams, 1990; Rothrock et al., 2003). This is the most significant ice thickness dataset today even though the coverage is sporadic and seasonal, inter-annual and spatial variations are poorly resolved (McLaren et al., 1992). Therefore, significant interest is being paid to alternative methods for monitoring sea ice thickness such as laser and radar altimetry (Kwok et al., 2004; Laxon et al., 2003; Wingham, 1999). However, estimating sea ice thickness by measuring its freeboard is disputed for two reasons: 1) the ice floe is not in hydrostatic equilibrium on a point-by-point basis. *"Therefore the relief of the underside of the ice and its thickness cannot be judged by the relief of the upper surface of the ice."* (Doronin & Kheisin, 1977), and 2) *"... to estimate the ice surface h_t and then multiply by ... 10 to obtain thickness h introduces unsatisfactory errors."* (Rothrock, 1986). Indeed, simple calculations of sea ice buoyancy show that the freeboard, in addition to thickness, is also a function of snow density and thickness and ice density. If these additional snow and ice properties are known, the error due to buoyancy can be reduced and it can be argued that although the floe is not in hydrostatic equilibrium on small scales there is a correlation between freeboard and ice thickness on larger scales. Nevertheless, to further reduce the error to "acceptable" levels (see 2 above) it is also necessary to minimize the freeboard measurement error. This paper addresses the latter by using a radiative transfer backscatter model for identifying sensitivities of the space borne radar altimeter

effective scattering surface depth used for snow/ice surface elevation and freeboard measurements.

Laboratory experiments, for dry snow on smooth sea ice, suggest that the total nadir looking radar backscatter is dominated by ice surface scattering and that snow and ice volume scattering are negligible (Beaven et al., 1995). Our model reproduces these observations. Yet the link between the backscatter mechanisms and the effective scattering surface is not established experimentally. The radiative transfer backscatter model is used to simulate the sea ice radar altimeter effective scattering surface variability as a function of a seasonal snow cover. The model is described in Tonboe et al. (2006) and hereafter called the backscatter model. Snow and ice profiles collected during the GreenICE project are used as input to the backscatter model and output from a mass and thermodynamic sea ice model (Tonboe, 2005) is used to assess the seasonal variability of these parameters in the central Arctic Ocean. This model is hereafter called the thermodynamic model.

Nadir looking radar backscatter
Surface scattering dominates backscatter in sea ice for a space borne Ku-band radar altimeter (Beaven et al., 1995). The nadir looking surface backscatter is a function of the nadir reflection coefficient $|R(0)|$ and the surface roughness (flat-patch area) F (Fetterer et al., 1992), i.e.

$$\sigma_{surf} = 0.9F\left|R(0)\right|^2 \frac{H}{u\tau}, \qquad (1)$$

where H is the satellite height, u the pulse propagation speed (speed of light in air, snow and ice) and τ the pulse length. A typical value for snow permittivity is about 1.5 and about 3.5 for sea ice (Ulaby et al., 1986). The reflectivity at the air/snow interface and the snow/ice interface is then about 0.1 and 0.2 respectively. Not accounting for extinction, this makes the ice surface backscatter nearly 5 times larger than snow surface backscatter using Eq. 1 (the same roughness for snow and ice). The dry snow permittivity and surface reflection coefficient is primarily a function of snow density. The relative importance of the snow surface backscatter is influenced by snow surface density, snow and ice surface roughness (F), snow extinction (deep snow and large scatterers or liquid water/ brine in the snow), and ice density and salinity. These parameters and processes are described in the backscatter model.

Snow on sea ice energy and mass balance
During precipitation events, the density of new snow is primarily a function of air temperature and wind speed (Jordan et al., 1999), and the snow gradually increases in density after deposition (Sturm & Holmgren, 1998). New snow is usually fine grained but the result of snow metamorphosis is always snow grain growth. The snow grains grow in dry snow as a function of temperature, temperature gradient, density and time (Marbouty, 1980). The short wave radiation snow albedo and extinction coefficient are functions of density and density and grain size respectively. The thermal snow conductivity is a function of density and temperature and these snow parameters are therefore important for the snow and ice energy balance. Both the thermal conductivity and specific heat of snow and ice are functions of temperature and the thermodynamic model therefore uses a finite difference scheme with a 10-minute time step.

2 RESULTS AND DISCUSSION

Simulated return pulse power for two measured snow and ice profiles

During the 2003 GreenICE campaign, two snow and first-year ice microphysical and temperature profiles were measured in Fram Strait near 76.26ºN, 23.28ºE. The ice thickness in the two profiles was identical (1.5m) while the snow thicknesses are 7cm and 36cm respectively. These profiles shown in Table 1 were used as input to the backscatter model and the simulated return pulse power is shown in Fig. 1. Surface roughness was not measured in the field and all layers have been assigned an equal flat-patch area of 1%.

Table 1. Snow and ice parameters used as input to the backscatter model: Temperature, T, Density, Layer thickness, correlation length (a measure of scatterer size) p_{ec} salinity S.

Thin snow profile

Layer No.	T [K]	Dens. [kg/m^3]	Thick [m]	p_{ec} [mm]	S [ppt]	Type
1	254	400	0.04	0.07	0.10	snow
2	257	250	0.03	0.15	0.10	snow
3	259	920	0.05	0.19	7.00	ice
4	264	920	1.45	0.17	7.00	ice

Thick snow profile

Layer No.	T [K]	Dens. [kg/m^3]	Thick [m]	p_{ec} [mm]	S [ppt]	Type
1	252	300	0.140	0.07	0.00	snow
2	262	920	0.002	0.10	0.00	snow
3	262	500	0.160	0.10	0.00	snow
4	265	300	0.060	0.15	0.00	snow
5	265	920	0.050	0.22	13.60	ice
6	267	920	0.100	0.21	11.30	ice
7	264	920	1.350	0.17	7.00	ice

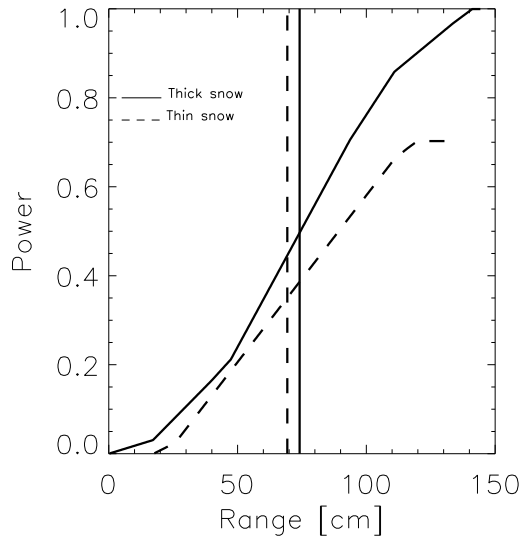

Figure 1. The simulated return pulse power as a function of apparent range. The vertical solid and dashed lines show the effective scattering surface. The thin (7cm) and thick (36cm) snow profiles shown in Tab. 1 are used as input.

The snow freeboards of the thick and the thin snow profile are 34cm and 17cm respectively giving the thick snow profile if in equilibrium (snow thickness 36cm) a slightly negative ice freeboard. The brine in the thin snow profile increases attenuation and reduce the total backscatter coefficient by 1.8dB compared to the thick snow profile with no brine. We simulate the water as a dielectric slab at sea level and compare this simulated range measurement with the effective scattering surfaces of the two snow/ice profiles. The simulated effective scattering surface for the thin snow profile is then 11.4cm above the water, i.e. just above the ice surface and the thick ice effective scattering surface is 6.6cm above the water inside the snow. The simulated range measurement is about 5cm longer for the thick snow profile than the thin snow profile while their respective ice surfaces are 12cm apart.

Seasonal variability of the effective scattering surface

Figure 2, snow cover vs. time, shows the simulated snow surface density and snow accumulation in a single profile on multiyear ice at 82.5ºN; 0.0ºE between Fram Strait and the North Pole during the 2000/2001 winter season. ECMWF reanalysis data are input to the thermodynamic model. The simulations begin with a bare ice surface on September 1, which is approximately the end of the melt season. The effective scattering surface is aligned with the ice surface on Sep. 1. Since the surface roughness is not a prognostic variable in the thermodynamic model, the flat-patch area is set to 1% for both the snow and ice. Ice growth is disabled during the simulation, i.e. the ice thickness is a constant 3.5m. Precipitation events of less than 1kg/m^2 (<1mm SWE) are not included. The backscatter model is coupled to the thermodynamic model and the seasonal variability of both the effective scattering surface and the penetration depth are shown. The penetration depth increase during winter as a function of decreasing ice temperature and brine volume. During most of the season, except for a period during Jan/Feb 2001, the simulated effective scattering surface follows the snow/ice interface closely. On Jan. 23. snow precipitation (Fig. 3) combined with winds of about 14m/s deposited a surface snow layer of 290kg/m^3 on top of the existing 130kg/m^3 surface layer. The new surface layer gradually compacted to 330kg/m^3. Later on Feb. 13. light snow fall combined with winds about 5m/s deposited a new surface snow layer of 190kg/m^3. These snow surface density variations explain the simulated effective scattering surface depth variations during this period. The effective scattering surface depth is affected by the distribution of backscattering magnitude between the snow and ice surface and the snow depth. The ice surface scattering magnitude is a function snow layer extinction and the parameters in Eq. 1. It seems from the single point simulation in figure 2 that the ½-power time is rather robust to the simulated natural snow cover variations during winter and that the effective scattering surface follows the ice surface closely. At the same time, there are several natural parameters not included in the model, which play a role for the effective scattering surface variability:

1. The snow and ice surface roughness. For a case in Tonboe et al. (2006) the simulated effective scattering surface depth varies by 12cm for varying roughness values. The different snow and ice roughnesses used represent extremes of this variation.

2. Saline snow. Saline snow on sea ice is common in the Antarctic. Though it is much less abundant in the Arctic even small amounts of brine can change the snow extinction significantly. An example is given in figure 1.

None of these important parameters are mapped systematically and it is therefore difficult to assess their spatial and temporal variability in the Arctic. The next section discusses future possibilities for snow and sea ice cover mapping by satellite.

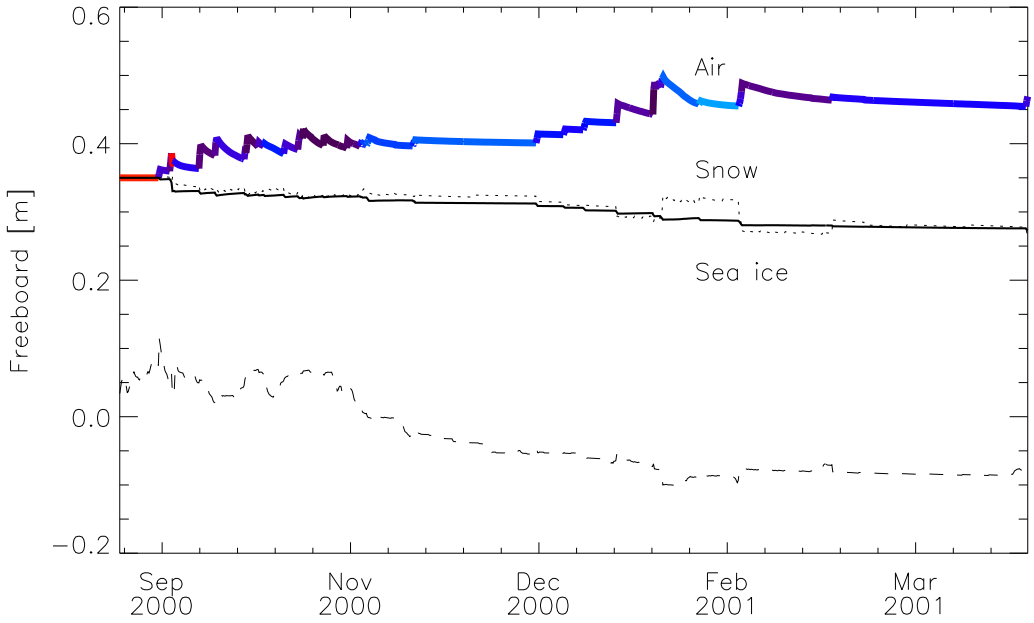

Figure 2. The simulated accumulation of snow in a single profile at 82.5ºN 0.0ºE during winter 2000/2001. The dashed line show the penetration depth at Ku-band and the dotted line show the depth of the effective scattering surface. The full line is the snow/ice interface. The colours of the snow surface line indicate the snow surface density.

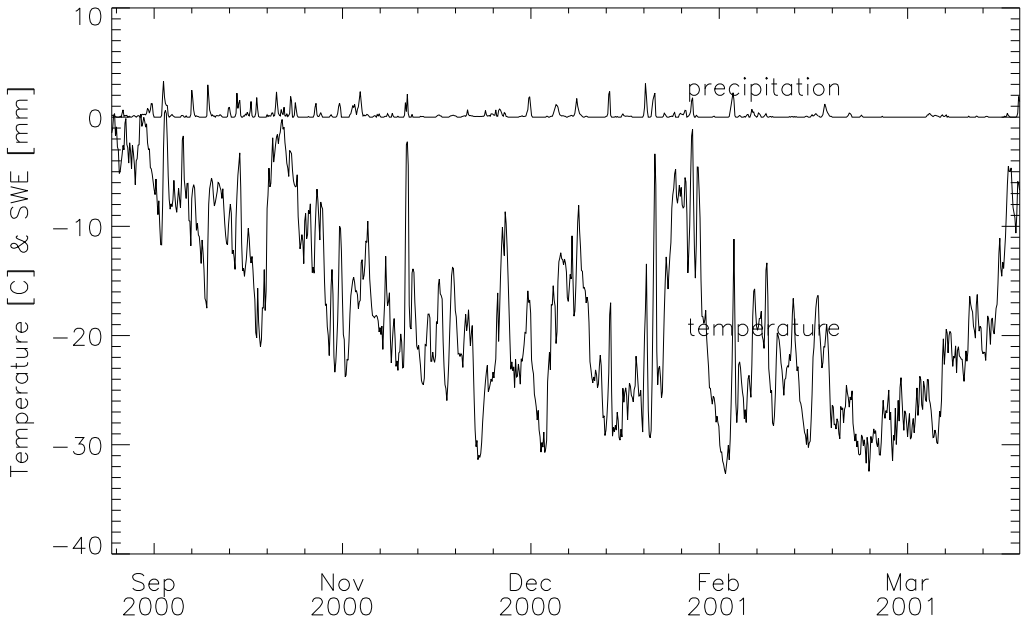

Figure 3. The ECMWF reanalysis air temperature and precipitation, (snow water equivalent, SWE), at 82.5ºN 0.0ºE, 2000/2001. These and other meteorological parameters are input to the thermodynamic model.

Need for hemispheric snow and ice mapping

Sea ice freeboard is a function of snow/ ice thickness and density. The effective scattering surface depth (dry snow) is primarily a function of snow surface density, snow depth and snow/ice surface roughness. These parameters are needed when estimating the radar altimeter effective scattering surface depth and further using the sea ice freeboard as a proxy for ice thickness. Sensitivity studies with quantification of the error is given in Tonboe et al. (2006).

Field campaigns and drifting stations have measured the sea ice snow cover during the last 50 years in the Arctic Ocean. These measurements are continued today during selected periods and locations e.g. the GreenICE project field activities 2003-2005. The measurements can be used to build a snow climatology (Warren et al., 1999). However using climatology to correct freeboard measurements makes it difficult to distinguish snow and ice thickness anomalies when interpreting satellite altimeter data. Algorithms for hemispheric mapping of snow on sea ice are therefore urgent and the possibilities for using satellite remote sensing for mapping snow depth and density as well as snow/ice surface roughness is discussed below.

Passive microwave radiometer data contain information on dry snow volume on land. High correlations are found locally between snow water equivalent (SWE) and microwave brightness temperature signatures (Mätzler et al., 2006). Markus & Cavalieri (1998) further derived an empirical relationship between snow cover depth on Antarctic sea ice and the spectral gradient between 19 and 37GHz in spaceborne SSM/I radiometer data. However, a universal SWE algorithm for snow on ice does not exist because the brightness temperature signature is also affected by layering, crusts and volume scattering (Mätzler et al., 2006). Pulliainen et al. (1999) demonstrated how physical models including several snow parameters might be inverted to derive single snow parameters (SWE) using spaceborne radiometer data. This approach seems promising also for future sea ice snow cover mapping. Surface roughness mapping using satellite data is even less established than snow cover mapping, but it is clear that the surface roughness play a significant role for C-band (e.g. Radarsat; Envisat ASAR; METOP ASCAT) and perhaps L-band (e.g. ALOS-PALSAR) SAR and scatterometer signatures (Onstott, 1992). Density of sea ice is related to the porosity and salinity (Doronin & Kheisin, 1977) and Ku-band and X-band backscatter is particularly sensitive to these ice parameters (Onstott, 1992). The QuikScat SeaWinds Ku-band scatterometer has now been operational since 1999 and proposed and near future satellite SAR missions will operate at these frequencies e.g. CoReH2O; TerraSAR. A significant effort is needed to bring these snow and ice cover mapping algorithms up to operational standard. Until these measures are taken the radar altimeter freeboard estimation errors remain high.

ACKNOWLEDGEMENTS

This work was supported by the European Commisions 5th framework programme; GreenICE (EVK2-2001-00280). Christian Haas of AWI measured and provided snow and ice profiles.

REFERENCES

Beaven, S. G., G. L. Lockhart, S. P. Gogineni, A. R. Hosseinmostafa, K. Jezek, A. J. Gow, D. K. Perovich, A. K. Fung, & S. Tjuatja. Laboratory measurements of radar backscatter from bare and snow-covered saline ice sheets. *International Journal of Remote Sensing 16*(5), 851-876, 1995.

Doronin, Y. P., & D. E. Kheisin. *Sea ice*. Amerind Publ. Co. Pvt. Ltd., New Delhi, 1977.

Fetterer, F. M., M. R. Drinkwater, K. C. Jezek, S. W. C. Laxon, R. G. Onstott, & L. M. H. Ulander, Sea ice altimetry. In: F. D. Carsey, Ed.,. *Microwave Remote Sensing of Sea Ice, Geophysical Monograph 68* (pp. 111-135). Washington DC: American Geophysical Union, 1992.

Jordan, R., E. Andreas, & A. Makshtas. Heat budget of snow covered sea ice at North Pole 4. *Journal of Geophysical Research 104*(C4), 7785-7806, 1999.

Kwok, R., H. J. Zwally, & D. Yi. ICESat observations of Arctic sea ice: A first look. *Geophysical Research Letters 31*, L16401, doi:10.1029/2004GL020309, 2004.

Laxon, S., N. Peacock & D. Smith. High interannual variability of sea ice thickness in the Arctic region. *Nature, 425*, 947-949, 2003.

Marbouty, D. An experimental study of temperature gradient metamorphism. *Journal of Glaciology 26*(94), 303-312, 1980.

Markus, T. & D. J. Cavalieri. Snow depth distribution over sea ice in the southern ocean from satellite passive microwave data. Antarctic Sea Ice, *Antarctic Research Series 74*, 19-39, 1998.

Mätzler, C., P.W. Rosenkranz, A. Battaglia and J.P. Wigneron, Eds., *Thermal Microwave Radiation - Applications for Remote Sensing, IEE Electromagnetic Waves Series*, London, UK, 2006.

McLaren, A. S., J. E. Walsh, R. H. Bourke, R. L. Weaver, & W. Wittmann. Variability in the sea-ice thickness over the North Pole from 1977 to 1990. *Nature 358*, 224-226, 1992.

Onstott, R. G. SAR and scatterometer signatures of sea ice. In: F.D. Carsey, Ed., *Microwave remote sensing of sea ice, Geophysical monograph 68* (pp. 73-104). Washington DC: American Geophysical Union, 1992.

Pulliainen, J., J. Grandell & M. Hallikainen. HUT snow emission model and its applicability to snow water equivalent retrieval. *IEEE Transactions on Geoscience and Remote Sensing 37*, 1378-1390, 1999.

Rothrock, D. A., J. Zhang & Y. Yu. The arctic ice thickness anomaly of the 1990s: A consistent view from observations and models. *Journal of Geophysical Research 108*(C3), 3083, doi: 10.1029/2001JC001208, 2003.

Sturm, M. & J. Holmgren. Difference in compaction behaviour of three climate classes of snow. *Annals of Glaciology 26*, 125-130, 1998.

Tonboe, R. A mass and thermodynamic model for sea ice. *Danish Meteorological Institute Scientific Report 05-10*, 2005.

Tonboe, R., S. Andersen, & L. Toudal Pedersen. Simulation of the Ku-band radar altimeter sea ice effective scattering surface. *IEEE Geoscience and Remote Sensing Letters 3(2), 237-240, 2006*.

Ulaby, F. T., R. K. Moore & A. K. Fung. *Microwave Remote Sensing, from Theory to Applications, vol. 3*. Dedham MA: Artech House, 1986.

Wadhams, P. Evidence for thinning of the Arctic ice cover north of Greenland. *Nature 345*, 795-797, 1990.

Warren, S. G., I. G. Rigor, N. Untersteiner, V. F. Radionov, N. N. Bryazgin, Y. I. Aleksandrov & R. Colony. Snow Depth on Arctic Sea Ice. *Journal of Climate 12*, 1814-1829, 1999.

Wingham, D. The first of the European Space Agency's opportunity missions: CryoSat. Earth *Observation Quarterly 63*, 21-24, 1999.